Multiband Wireless Power Transfer Using Time-frequency Modulated Metasurface

Huu Nguyen Bui, Van Truong Nguyen, and Jong-wook Lee

School of Electronics and Information

Kyunghee University

e-mail: *jwlee@khu.ac.kr, nguyencv90@khu.ac.kr, nguyenvantruong.bk@gmail.com*

Abstract

Multiple tiny devices use wireless power transfer (WPT) technology for charging their battery through the antenna coils that have a different operating frequency. So, a complex wave source requires a wide-band for charging those devices. In this work, we present an advanced method of WPT using metasurface. An experiment demonstrates that the controllable multiband WPT on the frequency regime from a monochrome wave source to many devices by using a time-frequency modulation metamaterial.

Ⅰ. Introduction

Metamaterials are new artificial subwavelength structures having unique electromagnetic properties no-existence in natural materials. The first one of metamaterial has a negative refractive index invented by sir Victor Veselago in 1968. He showed that exists a backward phase propagation in the metamaterials. This is contrary to wave propagation in naturally occurring materials [1].

Recently, the superior features of metamaterials have been used in WPT. Invented by sir Tesla, the WPT technology is grown and interested the scientist and engineers cause it has many applications ranging from short to long-distance and from very small implantable medical devices to industrial vehicles, with power transfer ranging from microwatts to hundreds of watts. So far, researchers have applicated metamaterial to reduce leaked power transfer to the load and demonstrated enhanced WPT efficiency at a larger distance [2].

WPT is a convenient way to transfer energy to devices, especially in medical applications, where the devices used are placed inside the body. However, the devices have a different frequency cause of the technical process [3].

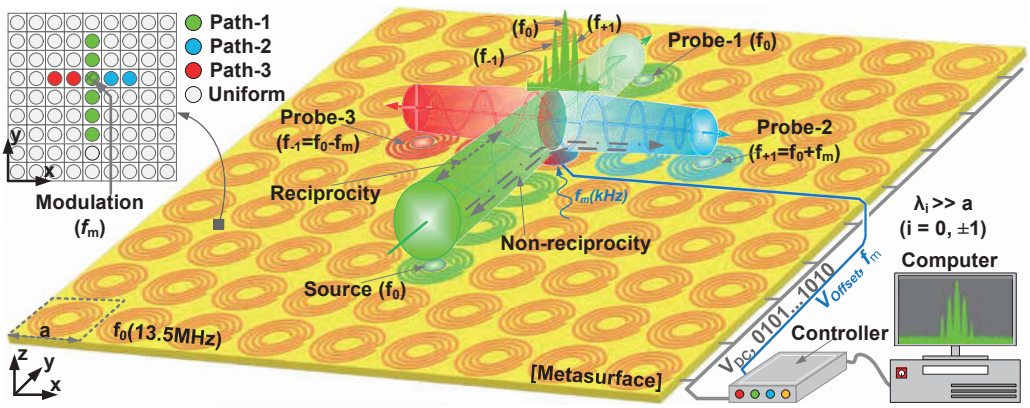

Fig.1. The schematic of time-frequency metasurface for multiple bands wireless power transfer system.

Various method for multiband WPT is presented [4-5]. However, those methods are the hybridization of nearly

resonance frequency [4]. For using different bandpasses, they need to switch the transfer frequency of the source device. Another research allows transfer power to the multi-receive device, but their system needs more RF source and multi-coils antenna [5].

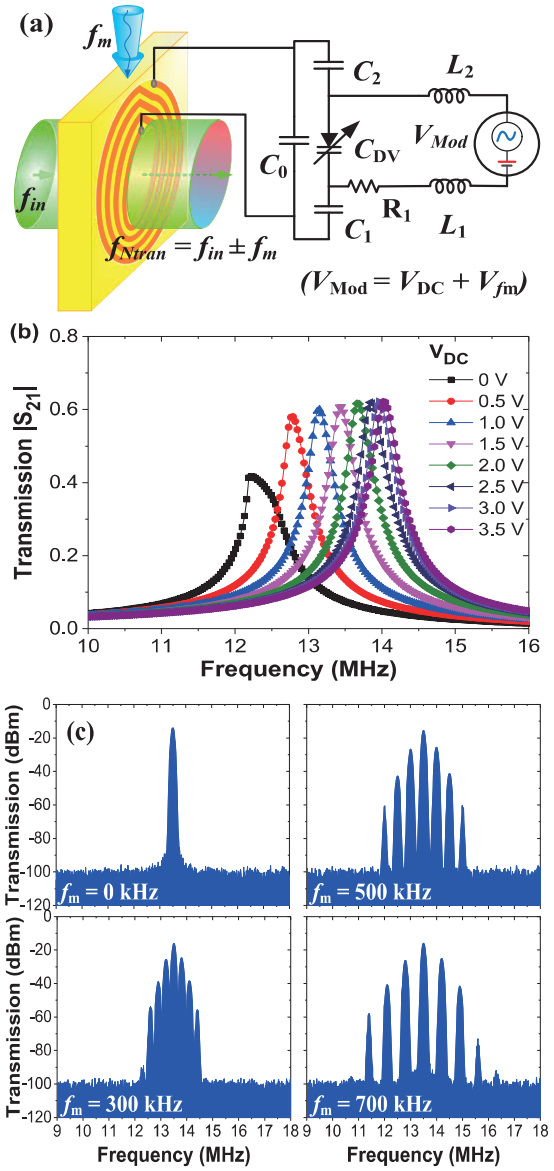

Fig.2. (a) The control circuit of the unit cell. (b) Resonance frequency responses of the unit cell as a function of the voltage control V_{DC}. (c) The transmitted power of the unitcell when are applied time-varying modulated frequency at 0, 300, 500, and 700 kHz.

The spacetime metamaterial is attractive to researchers because it has new features that previously unavailable materials such as beaking Lorentz reciprocity, controlling Doppler effect, beam manipulation, and so on [6].

In this paper, we propose a method using time-frequency modulation metamaterial for multiband WPT on non-reciprocity waveguides. This method, we only use an RF source with a center frequency, can be controlled and transferred power to multi-device, which have a different frequency.

II . Design

Fig. 1 shows the metasurface is realized by combining a 9x9 unit cells of the 4T-SR. By making the defected unit cells on the uniform metasurface, we set up three magnetic waveguides that operate at the difference frequency and called the path-1, path-2, and path-3. The unit cells of the path-1, path-2, and path-3 resonate at f_{p1} = 13.5 MHz, f_{p2} = 14 MHz, and f_{p3} = 13 MHz, respectively. On the uniform metasurface region, the unit cells resonate at f_U = 12.3 MHz.

Fig. 2(a) shows the schematic of the four-turn spiral resonator (4T-SR). The dimension of the 4T-SR is similar to the one used in previous work [7]. The activating circuit includes a significant capacitor C_0, two DC isolated capacitors C_1, C_2, two AC isolated inductors L_1, L_2, and a varactor DV having a variable capacitance C_{DV}, and a limited current resistor R_1. The varactor is biased by two signals, a static signal V_{DC}, which provides the required reverse bias and controls the static capacitance C_{DV}, and an RF signal V_{fm} with frequency f_m and amplitude V_m, providing the time modulation can be expressed as

$$V_{Mod} = V_{DC} + V_{fm}, \quad (1)$$

where V_{fm} is the modulated sinusoidal signal can be estimated using

$$V_{fm} = V_m sin(2\pi f_m t). \quad (2)$$

The RF signal V_{fm} applies on the circuit get a shifted phase of the incident wave.

$$\varphi_{tran} = \varphi_{in} + \varphi_m. \quad (3)$$

For the linear dispersion of the metamaterial, we

obtain the harmonic frequency N of the transmitted signal given by:

$$f_{Ntran} = f_{in} \pm N f_m \quad (4)$$

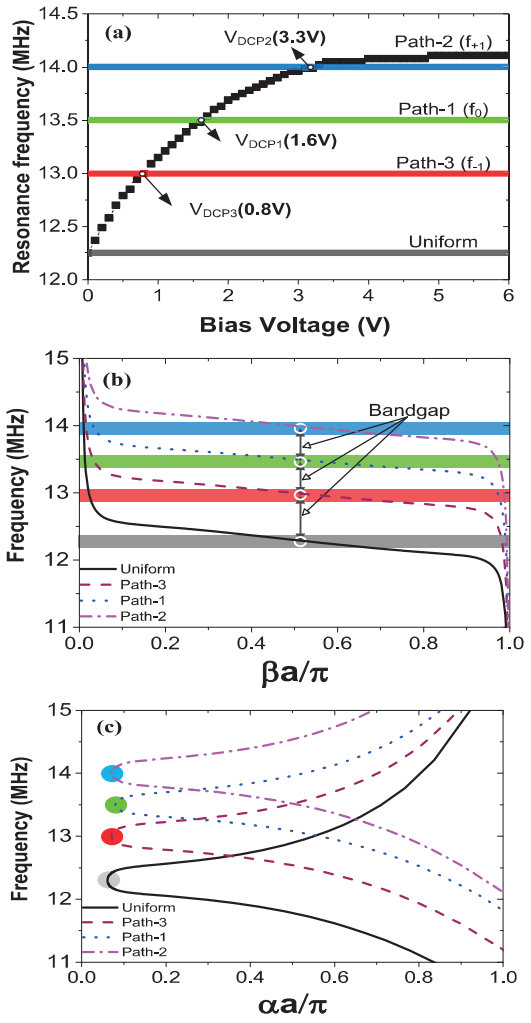

Fig. 3. (a) The illustration of three magnetic waveguides. (b) The response resonance frequency of the unit cells relatives the DC voltage bias of the three paths and uniform region. (c) the propagation constant, and (d) attenuation constant.

Fig. 2(c) shows the transmitted power of the unitcell when applying time-varying modulated frequency at 0, 300, 500, and 700 kHz, respectively.

Fig. 3(a) shows the metasurface without time-frequency modulation on the unit cells biased by the DC voltage. The unit cells of the bandgap region are provided by zero voltage. In contrast, the unit cells on the path-1, path-2, and path-3 are provided by V_{DCP1} = 1.6 V, V_{DCP2} = 3.3 V, and V_{DCP3} = 0.8 V, respectively.

Fig. 3(b) shows the propagation constant of the three paths. Through the bandgaps formed between the bandpass, the waves are not allowed to propagate on different paths. The source wave has a resonance frequency of 13.5 MHz is located at the terminal of the path-1 can be propagated to the probe-1 with smallest of attenuation constant of 0.08.

Fig. 3(c) shows the attenuation constants of this wave on the path-2 and path-3 are 0.53 and 0.55, respectively. Because of the high losses in the bandgap between the paths, the lower power of the wave resonant frequency of f_0 = 13.5 MHz is received at the probe-2 and probe-3. Furthermore, the loads are placed at the probe-2, and probe-3, which have self-resonant frequencies of 13 and 14 MHz, can not receive power at these frequencies from a monochrome source wave has a resonance frequency of 13.5 MHz.

Because the selective bandpass of the three magnetic waveguides, transmitting inductive wave from probe-2 and probe-3 at the frequency f_0 is not possible. This phenomenon relates to the non-reciprocity property of the metamaterial structure.

However, using a time-frequency modulation to a unit cell, which is noted as shown in Fig. 1, we can transfer power at multi bandpass simultaneously using a monochrome wave source. The demonstrated experimental results are presented in the next section.

III. Results

Fig. 4 shows the simulation results of the magnetic field distribution on the three paths at the phase of 0, 50, 100, and 150^0. Because of the resonance frequency of the three paths are different. The power from the source coil can not transfer to the probe-2 and probe-3. That is the reason why the magnetic field does not distribute on the path-2 and path-3.

Fig. 5 shows the measurement of the WPT system

using three magnetic waveguides on the uniform metasurface. The system includes three DC powers V_{DCP1}, V_{DCP2}, and V_{DCP3}, a time-frequency generator Vfm, an RF source, a signal analyzer, and the metasurface. The V_{DCP1}, V_{DCP2}, V_{DCP3} provide three bias voltages for the unit cells of the path-1, path-2, and path-3, and by changing voltage values, we can control the resonant frequency of the paths as shown in Fig. 3(a). The time-frequency generator V_{fm} provides a sinusoidal signal having a frequency fm in the kHz regime to the modulated unit cell. An RF source generates a monochrome wave at the MHz regime mode acts as a power source for transfer energy to the loads. The signal analyzer shows the power level that is captured by the probe.

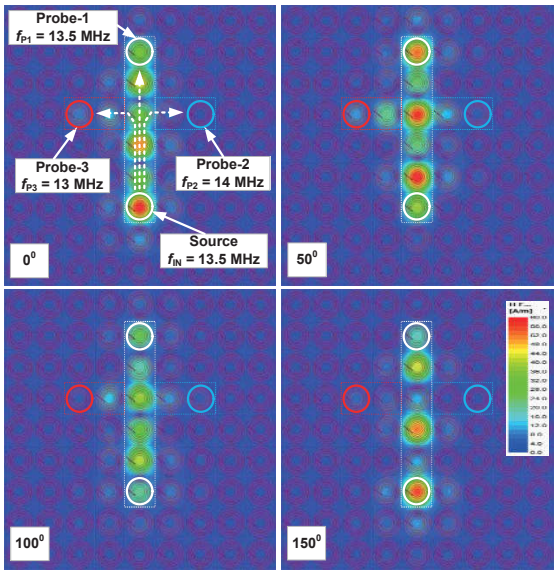

Fig. 4. The simulation results of the magnetic field distribution on the three paths at the phase of 0, 50, 100, and 150^0.

Figs. 6(b)-(d) show the results of transmitted power on the probe-1, probe-2, and probe-3 when we do not use time-frequency modulated at the cell (x, y) = (5, 6). The source coil is placed at the cell (x, y) = (5, 3) and the probe-1, 2, and 3 are placed at the cells (x, y) = (5, 8), (7, 6), and (3, 6), respectively. The number of cells from the source coil to the probes is the same as shown in Fig. 6(a). The input power has a magnitude of -11.5 dBm at the resonant frequency of f_{IN} = 13.5 MHz connected to the source coil.

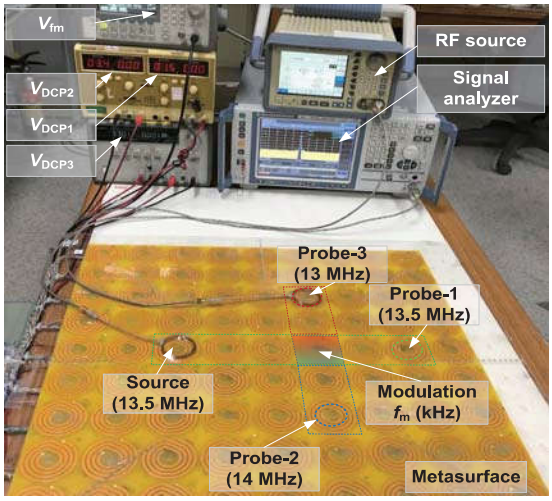

Fig. 5. The measurement system for multiple bandpass wireless power transfer.

Fig. 6(b) shows a transmitted power having a magnitude of -21.39 dBm at the resonant frequency f_{p1} = f_{IN} = 13.5 MHz is capture by probe-1. Figs. 6(c)-(d) show the magnitude of transmitted power on the probe-2 and 3 are -30.04 dBm and – 30.81 dBm at the resonant frequency f_{IN} = 13.5 MHz. At the resonant frequency of 13.5 MHz, the transmitted power on the probe-2 and probe-3 are smaller than on probe-1 because the source wave transferred to the probe-2 and probe-3 with a higher loss as shown in Fig. 3(c). Without time-frequency modulation, the probe-2 and -3 can not receive the power at the resonant frequency of 14 MHz and 13 MHz, respectively.

Figs. 6(f)-(h) show the results of transmitted power on the probe-1, probe-2, and probe-3 when we use time-frequency modulation. The sinusoidal signal V_{fm} has a frequency of 500 kHz, and the amplitude of V_m = 0.6 V generated by a time-frequency generator. This time-frequency modulation signal is sent to the cell (x, y) = (5, 6) shown in Fig. 6(e). The input power has a magnitude of -11.5 dBm at the resonant frequency of 13.5 MHz connects to the source coil.

By using time-frequency modulation, the multiband transmitted power is captured by the probe-1, probe-2, and probe-3. These results show a multiband pass that includes a center resonant frequency f_{IN} = 13.5 MHz, and the harmonic frequencies are defined by equation (4).

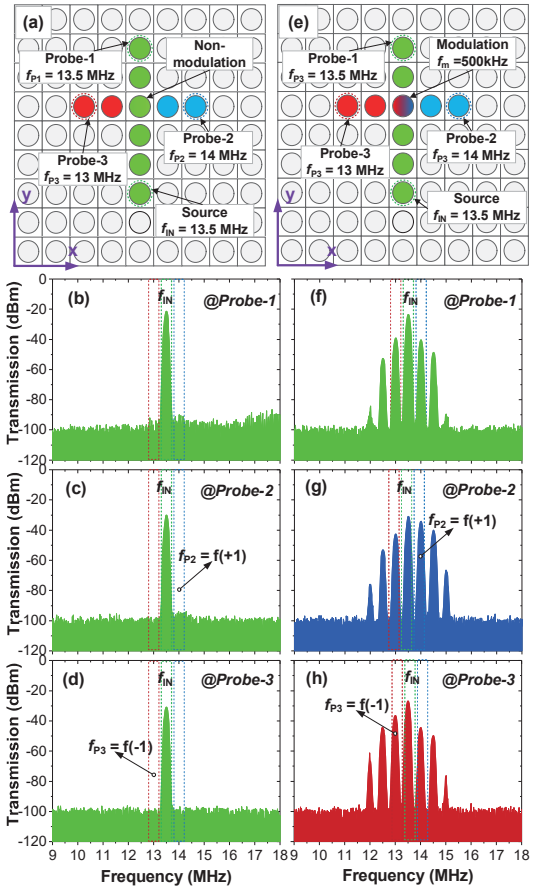

Fig. 6. The measurement of transmitted power. (a)-(d) the transmitted power from a wave source (13.5 MHz) to the probes without applying time-frequency modulation. (e)-(h) with using time-frequency modulation at 500 kHz.

Fig. 6(f) shows the multiband transmitted power on the probe-1. The transmitted power is -23. 59 dBm at f_{IN} = 13.5 MHz, and -40.4 dBm and -39.03 dBm at f(+1) = 14 MHz and f(-1) = 13 MHz, respectively.

Fig. 6(g) shows the multiband transmitted power on the probe-2. The transmitted power is -30. 91 dBm at fIN = 13.5 MHz, and -34.2 dBm and -42.63 dBm at f(+1) = 14 MHz and f(-1) = 13 MHz, respectively. On the probe-2, the transmitted power magnitude of harmonic frequency at f(+1) = 14 MHz is higher than on the probe-1 because path-2 has a resonant frequency of 14 MHz, so f(+1) transferred on this path with a smallest lossy.

Fig. 6(h) shows the multiband transmitted power on the probe-3. The transmitted power is -26. 78 dBm at fIN = 13.5 MHz, and -44.37 dBm and -36.48 dBm at f(+1) = 14 MHz and f(-1) = 13 MHz, respectively. On the probe-2, the transmitted power magnitude of harmonic frequency at f(-1) = 13 MHz is higher than on the probe-1 because path-3 has a resonant frequency of 13 MHz, so f(-1) transferred on this path with a smallest lossy.

IV. Conclusion

In this work, we investigate a new method of transferring and controlling multiple band power. The proposed method is achieved using a time-varying modulated frequency on metamaterial. By using this method, we can transfer the power to many devices having a difference operated frequency while using only one monochrome wave source. The proposed method can find useful applications demanding a small device, for example, future biomedical and biological applications.

REFERENCES

[1] V. G. Veselago, "Reviews of Topical Problems: the Electrodynamics of Substances with Simultaneously Negative Values of ε and μ ," *Sov. Phys. Usp.,* vol. 10, no. 4, p. R04, 1968.

[2] G. Lipworth, et al., "Magnetic metamaterial superlens for increased range wireless power transfer," *Sci. Rep.,* vol. 4, p. 3642, 2014.

[3] A. Kiourti and K. S. Nikita, "A review of in-body biotelemetry devices: Implantables, ingestibles, and injectables," *IEEE Trans. Biomed. Eng.*, vol. 64, no. 7, pp. 1422-1430, 2017.

[4] O. Jonah, S. V. Georgakopoulos, and M. M. Tentzeris, " Multiband wireless power transfer via resonance magnetic," *in 2013 IEEE Antennas and Propagation Society International Symposium (APSURSI)*, pp. 850-851, Orlando, USA, 2013.

[5] M. Liu and M. Chen, “Dual-Band Multi-Receiver Wireless Power Transfer: Architecture, Topology, and Control,” in *2019 IEEE Applied Power Electronics Conference and Exposition (APEC)*, pp. 851-859, Anaheim, USA, 2019.

[6] C. Caloz and Z. L. Deck-Léger, “Spacetime Metamaterials—Part I: General Concepts,” *IEEE Trans. Antennas Propag.,* vol. 68, no. 3, pp. 1569-1582, 2019.

[7] A. L. A. K. Ranaweera, T. S. Pham, H. N. Bui, V. Ngo, and J. W. Lee, “An active metasurface for field-localizing wireless power transfer using dynamically reconfigurable cavities,” *Sci. Rep.*, vol. 9, no.1, pp. 1-12, 2019.